Received: 6 December 2021 | Revised: 21 February 2022 | Accepted: 1 April 2022

DOI: 10.1002/jbt.23077

WILEY

DDX3X alleviates doxorubicin-induced cardiotoxicity by regulating Wnt/β-catenin signaling pathway in an in vitro model

Dandan Feng[1] | Jiang Li[1] | Liang Guo[2] | Jing Liu[3] | Shaochen Wang[4] | Xiuyuan Ma[1] | Yunxuan Song[4] | Ju Liu[3] | Enkui Hao[1]

[1]Department of Cardiology, Shandong Provincial Qianfoshan Hospital, Cheeloo College of Medicine, Shandong University, Jinan, China

[2]Department of Anesthesiology, The First Affiliated Hospital of Shandong First Medical University and Shandong Provincial Qianfoshan Hospital, Jinan, China

[3]Laboratory of Microvascular Medicine, Medical Research Center, Shandong Provincial Qianfoshan Hospital, The First Affiliated Hospital of Shandong First Medical University, Jinan, China

[4]Department of Cardiology, Shandong Provincial Qianfoshan Hospital, Shandong First Medical University, Jinan, China

Correspondence
Enkui Hao, Department of Cardiology, Shandong Provincial Qianfoshan Hospital, Cheeloo College of Medicine, Shandong University, 16766 Jingshi Rd, Jinan, Shandong 250012, China.
Email: haoenkui@sdu.edu.cn

Funding information
Science and Technology Project of Shandong Province, Grant/Award Number: 11731303; National Nature Science Foundation of China, Grant/Award Number: 81873473; Academic Promotion Program of Shandong First Medical University, Grant/Award Number: 2019QL014; Jinan City's Science and Technology Innovation Program of Clinical Medicine, Grant/Award Number: 202019175

Abstract

The life-threatening adverse effects of doxorubicin (Dox) caused by its cardiotoxic properties limit its clinical application. DDX3X has been shown to participate in a variety of physiological processes, and it acts as a regulator of Wnt/β-catenin signaling. However, the role of DDX3X in Dox-induced cardiotoxicity (DIC) remains unclear. In this study, we found that DDX3X expression was significantly decreased in H9c2 cardiomyocytes treated with Dox. *Ddx3x* knockdown and RK-33 (DDX3X ATPase activity inhibitor) pretreatment exacerbated cardiomyocyte apoptosis and mitochondrial dysfunction induced by Dox treatment. In contrast, *Ddx3x* overexpression ameliorated the DIC response. Moreover, Wnt/β-catenin signaling in cardiomyocytes treated with Dox was suppressed, but this suppression was reversed by *Ddx3x* overexpression. Overall, this study demonstrated that DDX3X plays a protective role in DIC by activating Wnt/β-catenin signaling.

KEYWORDS
apoptosis, cardiotoxicity, DDX3X, doxorubicin, Wnt/β-catenin

1 | INTRODUCTION

Doxorubicin (Dox) is a highly effective antineoplastic agent against various malignancies, such as lung cancer, breast cancer, leukemia, and lymphoma.[1,2] However, the cardiotoxic side effects of Dox, including acute and chronic dose-dependent cardiotoxicity and heart failure, limit its clinical application.[3] A number of factors participate in the pathogenesis of Dox-induced cardiotoxicity (DIC), including oxidative stress, apoptosis, and intracellular calcium dysregulation.[4] However, the underlying mechanisms remain largely unknown.

Abbreviations: ANOVA, analysis of variance; CCK-8, cell counting Kit-8; DIC, dox-induced cardiotoxicity; Dox, doxorubicin; PVDF, polyvinylidene difluoride; qRT-PCR, quantitative real-time polymerase chain reaction; ROS, reactive oxygen species; SDS-PAGE, sodium dodecylsulfate-polyacrylamide gel electrophoresis.

Therefore, there is an immediate need to investigate potential intervention targets and propose effective therapeutic strategies to mitigate DIC.

A large body of evidence has shown that Wnt/β-catenin signaling plays a crucial role in numerous pathological processes and maintains adult tissue homeostasis by regulating cell proliferation, differentiation, genetic stability, and apoptosis.[5] Under resting conditions, cytosolic β-catenin is rapidly degraded,[6] and activation of the Wnt signaling pathway contributes to the stabilization and accumulation of cytosolic β-catenin.[7] Subsequently, active β-catenin translocates to the nucleus and promotes pro-survival and antiapoptotic gene expression by interacting with TCF-LEF transcription factors.[8] The protective effects of Wnt/β-catenin signaling have been widely elucidated. For instance, the activation of Wnt/β-catenin signaling significantly reduces reactive oxygen species (ROS) and apoptosis induced by intestinal ischemia/reperfusion (I/R) injury.[9] β-catenin is conducive to endothelial survival by promoting antiapoptotic gene expression and regulating eNOS activity.[10] Statins alleviate reoxygenation-induced cardiomyocyte apoptosis by promoting the accumulation and nuclear translocation of cytosolic β-catenin.[11]

DDX3 belongs to a highly conserved family of DEAD-box proteins, a large family of RNA helicases that are widely expressed in eukaryotes.[12] The human genome encodes two functional *Ddx3* homologs, *Ddx3x* and *Ddx3y*, which are localized on the X and Y chromosomes, respectively.[13–15] DDX3Y is expressed only in spermatocytes and plays a vital role in spermatogenesis, whereas DDX3X is expressed ubiquitously and functions in somatic tissues.[16] DDX3X has been shown to be involved in a variety of biological processes, such as RNA metabolism, innate immune response, stress responses, and tumor progression.[17] In addition, DDX3X has been shown to regulate Wnt/β-catenin signaling in mammalian cells by directly binding to CK1ε and stimulating its kinase activity, thereby promoting the accumulation and nuclear translocation of cytoplasmic β-catenin.[18] However, the role of DDX3X in DIC remains largely unknown.

In this study, we sought to determine the role of DDX3X in the DIC pathophysiology. The results manifested that DDX3X expression was remarkably downregulated in H9c2 cells treated with Dox. A series of results indicated that DDX3X exerted a protective effect against DIC by positively regulating Wnt/β-catenin signaling. This study provides new insights into the mechanisms of DIC and potential therapeutic targets against this disease.

2 | MATERIALS AND METHODS

2.1 | Cell culture and reagents

Rat embryonic ventricular myoblastic H9c2 cells were bought from the National Collection of Authenticated Cell Culture (https://cellbank.org.cn), were cultured with DMEM (Cat. No. 12800017, Gibco) supplemented with 10% fetal bovine serum (No. 04-001-1ACS, Biological Industries), 1.5 g/L $NaHCO_3$ (Cat. No. A500873), and 1% Penicillin-Streptomycin liquid (Cat. No. P1400) in a humidified atmosphere of 95% air and 5% CO_2 at 37°C. Dox was obtained from MedChemExpress (Cat. No. HY-15142) and used at the concentration of 2 μM.[19] RK-33 was purchased from Selleck.cn (Cat. No. S8246) and used at the concentration of 7.5 μM. LiCl was bought from Solarbio (Cat. No. C8380) and used at the concentration of 20 mM.

2.2 | Transfection of *Ddx3x* siRNA

H9c2 cells at 50%–60% confluence were transiently transfected with 50 nM *Ddx3x* siRNA and scramble siRNA (GENERAL BIOL) by using Lipofectamine™ 3000 reagent (Cat. No. L3000015, Invitrogen) according to the manufacturer's instructions. Nontargeting scramble siRNA was used as negative control. After transfection for 6–8 h, the serum-free medium was changed with DMEM medium containing serum. After transfection for 24 h, the effect of gene knockdown was detected by RT-qPCR. The sense and antisense siRNA sequences are listed in Table 1.

2.3 | Transfection of *Ddx3x* pcDNA3.1-3xFlag-C plasmids

Ddx3x pcDNA3.1-3xFlag-C plasmids and negative control plasmids were obtained from Research Cloud Biology, Inc. H9c2 cells at 70%–80% confluence were transfected with 2.5 μg *Ddx3x* pcDNA3.1-3xFlag-C plasmids and negative control plasmids by using Lipofectamine™ 3000 reagent (Cat. No. L3000015, Invitrogen) according to the manufacturer's instructions. After transfection for 24 h, H9c2 cells were treated with 2 μM Dox for another 24 h.

2.4 | Western blots and antibodies

Protein samples were extracted using RIPA agent (Cat. No. P0013B) and quantified by the bicinchoninic acid assay kit (Cat. No. P0012). 20 μg of total proteins were separated by 10% and 15% SDS-PAGE (meilunbio) gel and subsequently transferred onto PVDF membranes

TABLE 1 Sense and antisense siRNA strand sequences

Gene	Sequence (5′–3′)
DDX3X siRNA	5′-GGAGGAUUUCUUAUACCAUTT-3′
Sense strand	
DDX3X siRNA	5′-AUGGUAUAAGAAAUCCUCCTT-3′
Antisense strand	
Control siRNA	5′-UUCUCCGAACGUGUCACGUTT-3′
Sense strand	
Control siRNA	5′-ACGUGACACGUUCGGAGAATT-3′
Antisense strand	

(Cat. No. IPVH00010). The PVDF membranes were blocked with 5% defatted milk for 1 h and subsequently incubated with specific primary antibodies at 4℃ overnight. Then, the PVDF membranes were incubated with Goat Anti-rabbit IgG HRP-linked secondary antibody (Cat. No. A21020, Abbkine Scientific Co., Ltd, 1:10,000) for 1 h. The immunoblots were visualized using chemiluminescent HRP substrate (Cat. No. WBKLS0100). The bands were detected using a chemiluminescent analyzer (ProteinSimple, USA) and the intensity analysis was performed by ImageJ v1.8.0.112 software (National Institutes of Health). GAPDH acts as the internal control. The primary antibodies were used as follows: GAPDH Rabbit Polyclonal antibody (Cat. No. 10494-1-AP, Proteintech, 1:8000), DDX3 Rabbit Polyclonal antibody (Cat. No. 11115-1-AP, Proteintech, 1:1000), Beta Catenin Rabbit polyclonal antibody (Cat. No. 51067-2-AP, Proteintech, 1:1000), Caspase 3/p17/p19/Rabbit Polyclonal antibody (Cat. No. 19677-1-AP, Proteintech, 1:1000).

2.5 | Cell viability assay

H9c2 cells were seeded onto 96-well plates (Cat. No. 310109008, LabServ) with six replicate wells for each treatment condition at a density of 1000 cells/well and cultured for 24 h before the corresponding treatment. After treatment, Cell Counting Kit-8 (CCK-8) reagent (Cat. No. K1018, APExBIO Technology LLC) was added into cell culture medium. Then, H9c2 cells were incubated at 37℃ for 4 h. The OD (optional density) value was captured using an enzyme-labeled instrument (BioTek Instruments, Inc.) at a wavelength of 450 nm. The H9c2 cells viability was evaluated by relative absorbance.

2.6 | Quantitative real-time polymerase chain reaction (qRT-PCR)

Total RNA from H9c2 cells was isolated using RNA isolater Total RNA (Cat. No. R401-01, Vazyme Biotech Co., Ltd.). cDNA was prepared using the HiScript III RT SuperMix for qPCR (+gDNA wiper) (Cat. No. R323-01, Vazyme Biotech Co., Ltd.) according to the manufacturer's instructions. Primer sequences were obtained from Accurate Biotechnology (Hunan) Co., Ltd. qRT-PCR was carried out with cDNA using ChamQ Universal SYBR qPCR Master Mix (Cat. No. Q711-02, Vazyme Biotech Co., Ltd.). The amplification conditions were 30 s at 95℃, then followed by 40 cycles of 10 s at 95℃ and 30 s at 60℃. Thermal cycling and fluorescence detection were conducted using a CFX96 Real-Time PCR Detection System (Bio-Rad Laboratories, Inc.). The transcriptional level of DDX3X were normalized to GAPDH. The primer sequences used for qPCR are listed in Table 2.

2.7 | Assessment of apoptosis by flow cytometric analysis

Fow cytometry analysis was conducted to detect H9c2 cells apoptosis using an Annexin V-FITC/PI Apoptosis Detection kit (Cat. No. MAO220-2; meilunbio). After different treatment, H9c2 cells were digested with 0.25% Trypsin-no EDTA (Cat. No. MA0234) and collected after centrifuged at 1000 x g for 5 min. Then, the cells were washed with precooling PBS (Cat. No. P1020) three times. Next, cells were re-suspended using 1X Binding buffer containing 5 μl of Annexin-V and 5 μl PI. The mixture was incubated at room temperature for 15 min in the dark. The apoptotic cells were analyzed using BD FACSAria™ II Cell Sorter (BD Biosciences). The data were analyzed using FlowJo_v10.6.2. Early and late apoptotic cells were used to calculate the apoptotic rate.

2.8 | Mito-tracker red CMXRos and hoechst 33342 staining to detect cell apoptosis

Mito-Tracker Red CMXRos (Cat. No. C1049B, Beyotime Biotechnology) and Hoechst 33342 Staining Solution for Live Cells (Cat. No. C1028, Beyotime Biotechnology) were used to identify the apoptotic cells. After different treatments, H9c2 cells were incubated with DMEM containing 200 nM Mito-Tracker Red CMXRos and 1X Hoechst 33342 Staining Solution at 37℃ for 30 min in the dark. Fluorescence images were scanning using a fluorescence microscope (Leica, Germany).

TABLE 2 Primer sequences used for quantitative polymerase chain reaction

Gene	Sequence	Product size (bp)	TM (℃)
DDX3X-Rat			
F:	5′-AAACCTTGGTCTTGCCACCTC-3′	21	57.57
R:	5′-CCACGGCTGCTACCCTTATAG-3′	21	59.52
GAPDH-Rat			
F:	5′-GTATTGGGCGCCTGGTCACC-3′	20	61.55
R:	5′-CGCTCCTGGAAGATGGTGATGG-3′	22	61.85

Abbreviations: F, forward; R, reverse; bp, base pair; TM, melting temperature.

2.9 | Statistical analysis

Statistical analysis was conducted using GraphPad Pro Prism 8.0 software (GraphPad Software, Inc.). Statistical significance was evaluated by Unpaired Student's test for two groups and one-way analysis of variance (ANOVA) for multiple groups. Every experiment was repeated three times. The data are presented as the mean ± SEM. Statistical significance was regarded as $p < 0.05$.

3 | RESULTS

3.1 | DDX3X expression was downregulated in DIC in H9c2 cells

H9c2 cells were treated with 2 μM Dox for the indicated time periods. As shown in Figure 1A, the activation level of Caspase-3 notably increased after Dox treatment for 24 h. Flow cytometric analysis showed that the apoptosis ratio of H9c2 cardiomyocytes was remarkably elevated after Dox treatment for 24 h (Figure 1B). RT-qPCR and western blot analysis were used to evaluate the expression of DDX3X. As presented in Figure 1C, the results of RT-qPCR showed that DDX3X mRNA levels were notably decreased after Dox treatment. The Western blot analysis results suggested that DDX3X protein levels were significantly reduced after exposure to Dox for 24 h (Figure 1D). These results indicate that DDX3X expression was decreased in H9c2 cells treated with Dox.

3.2 | *Ddx3x* knockdown and pharmacological inhibition of DDX3X both exacerbated Dox-induced cardiomyocyte apoptosis

To determine whether DDX3X plays a role in Dox-induced cardiomyocyte apoptosis, *Ddx3x* siRNA was used to silence DDX3X expression in H9c2 cells. RT-qPCR analysis was used to determine the efficiency of *Ddx3x* siRNA transfection (Figure 2A). As shown in Figure 2B, compared to the control group, *Ddx3x* knockdown clearly increased the activation level of caspase-3 in H9c2 cells treated with Dox. Flow cytometric analysis, Mito-Tracker Red CMXRos and Hoechst 33342 staining, and cell viability assay results also indicated that DDX3X deficiency aggravated the cardiotoxic response of H9c2 cells treated with Dox (Figure 2C–E). To investigate whether DDX3X RNA helicase is involved in the mechanism of DIC, H9c2 cells were pretreated with RK-33, a DDX3X ATPase activity inhibitor. As shown in Figure 2F, RK-33 pretreatment did not affect DDX3X expression in H9c2 cells treated with or without Dox, and it significantly elevated the activation level of Caspase-3 in Dox-treated H9c2 cells. Mito-Tracker Red CMXRos and Hoechst 33342 staining

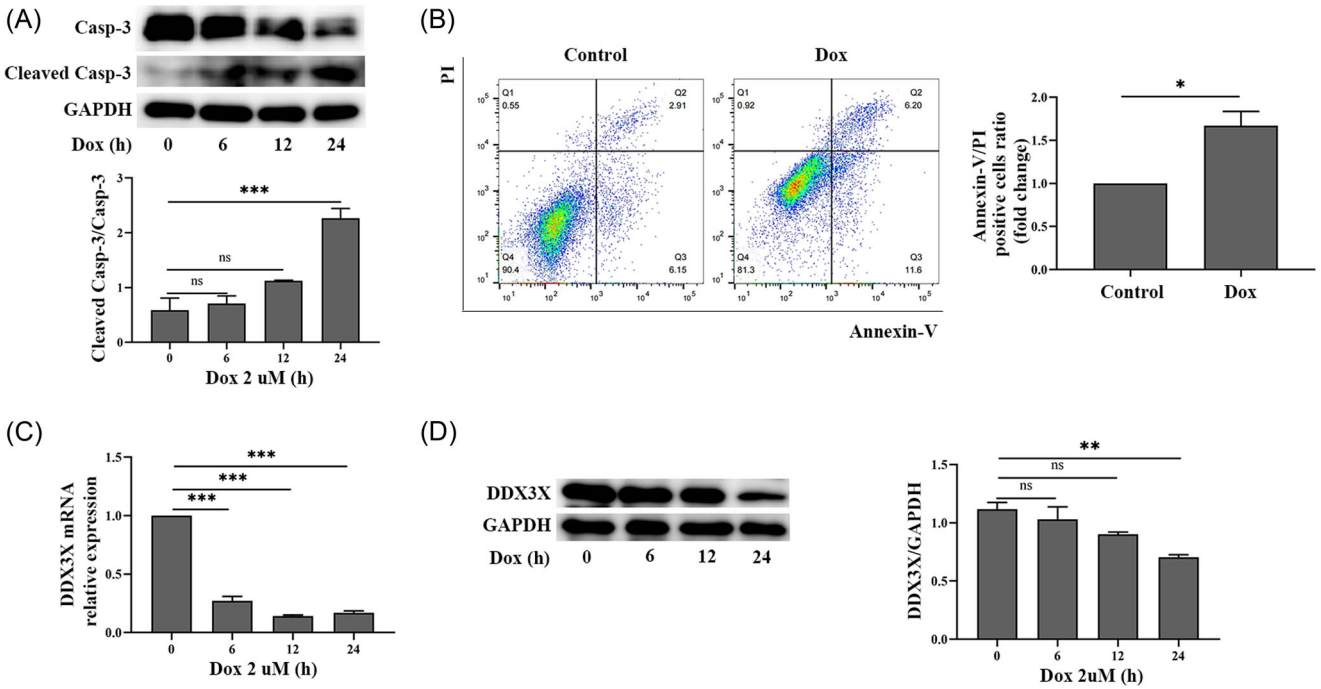

FIGURE 1 DDX3X expression in Dox-induced cardiotoxicity in H9c2 cells. (A) The protein level of Casp-3 and cleaved Casp-3 in H9c2 cells treated with Dox (2 μM) for 0, 6, 12, and 24 h were detected by Western blot. The data are presented as means ± SEM. ns, $p \geq 0.05$ refers to not significant; ***$p < 0.001$. (B) The apoptosis ratio of H9c2 cardiomyocytes was measured by flow cytometric analysis. The data are presented as means ± SEM. *$p < 0.05$. (C) The mRNA expression of DDX3X in H9C2 cardiomyocytes treated by Dox (2 μM) for 0, 6, 12, and 24 h were detected by RT-qPCR. The data are presented as means ± SEM. ***$p < 0.001$. (D) The protein level of DDX3X in H9C2 cardiomyocytes stimulated by Dox (2 μM) for 0, 6, 12, and 24 h. The data are presented as means ± SEM. ns, $p \geq 0.05$ refers to not significant; **$p < 0.01$

results also showed that RK-33 pretreatment notably increased the apoptosis ratio of H9c2 cells after Dox treatment (Figure 2G). Taken together, these results suggested that DDX3X protein deficiency and inhibition of DDX3X ATPase activity aggravated DIC in H9c2 cells.

3.3 | *Ddx3x* overexpression ameliorated Dox-induced cardiomyocyte apoptosis

Ddx3x pcDNA3.1-3xFlag-C plasmids were transduced into H9c2 cardiomyocytes. The efficiency of the *Ddx3x* plasmid transfection was

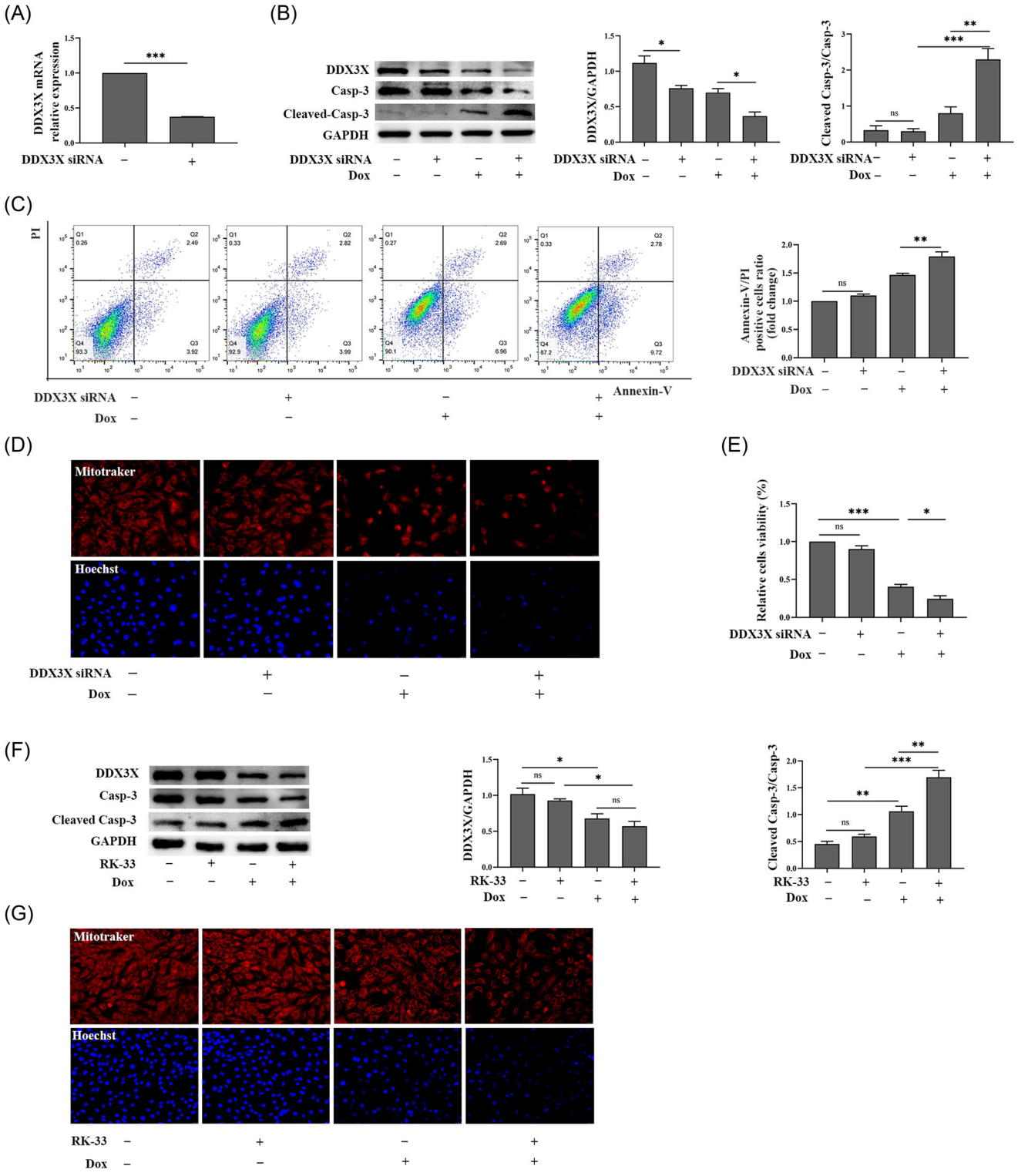

FIGURE 2 (See caption on next page)

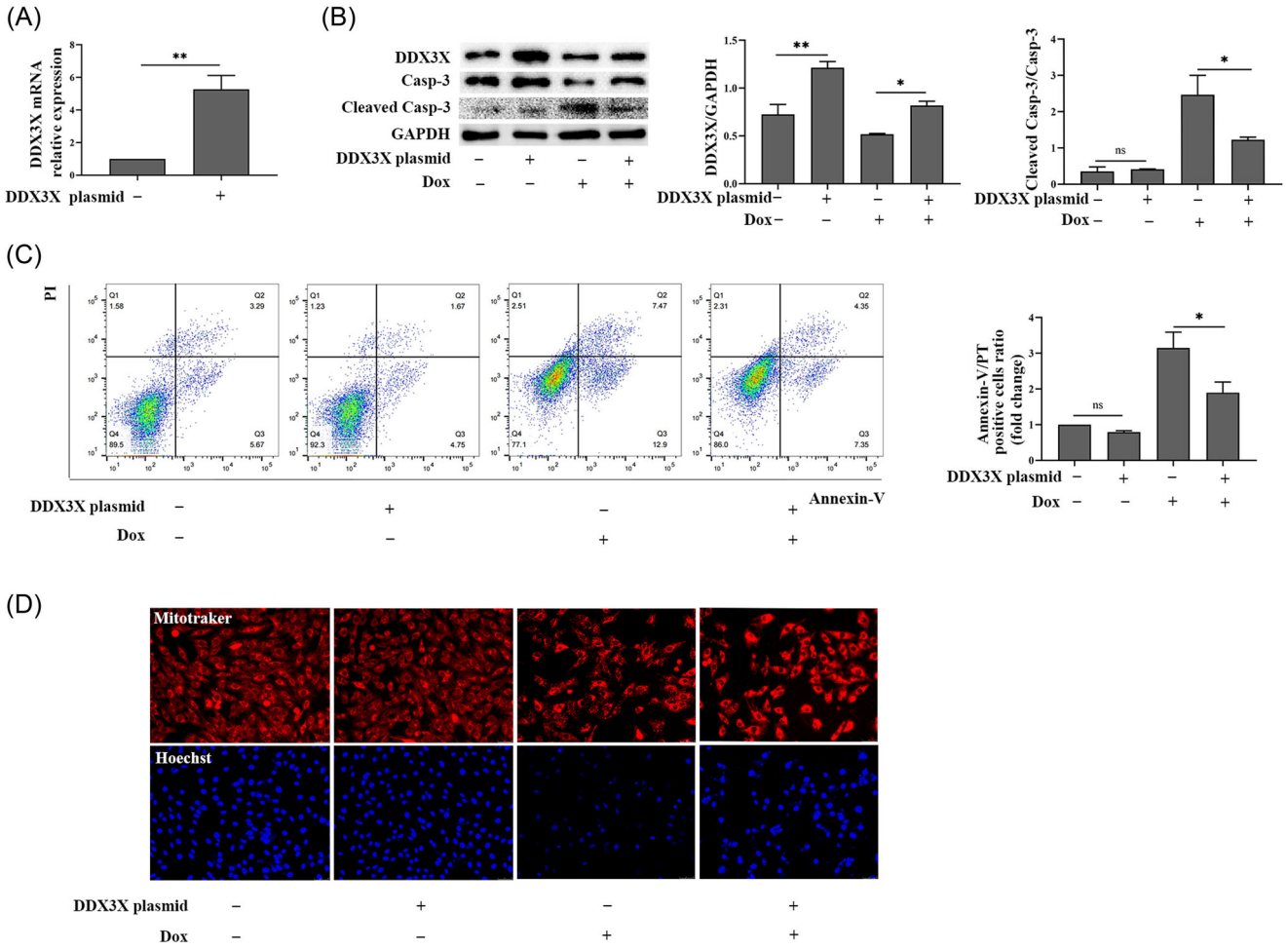

FIGURE 3 *Ddx3x* overexpression ameliorated Dox-induced cardiomyocyte apoptosis. "+" symbol denotes presence and "−" symbol denotes absence of the corresponding treatment condition. (A) The RT-qPCR analysis evaluated the efficiency of *Ddx3x* plasmids transfection. Data are presented as means ± SEM. $^{**}p < 0.01$. (B) The protein level of DDX3X, Casp-3, and cleaved Casp-3 in H9c2 cells treated with Dox (2 μM) following *Ddx3x* plasmids transfection. Data are presented as means ± SEM. ns, $p \geq 0.05$ refers to not significant; $^{*}p < 0.05$; $^{**}p < 0.01$. (C) Flow cytometric analysis detected the apoptosis ratio of H9c2 cardiomyocytes treated with Dox (2 μM) following *Ddx3x* plasmids transfection. The data are presented as means ± SEM. ns, $p \geq 0.05$ refers to not significant; $^{*}p < 0.05$. (D) Mito-Tracker Red CMXRos and Hoechst 33342 staining were detected respectively mitochondrial morphology and nuclear condensation of H9c2 cells treated with Dox (2 μM) following *Ddx3x* plasmids transfection. Scale bar = 50 μm

FIGURE 2 *Ddx3x* knockdown and pharmacological inhibition of DDX3X both exacerbated Dox-induced cardiomyocyte apoptosis. "+" symbol denotes presence and "−" symbol denotes absence of the corresponding treatment condition. (A) The RT-qPCR analysis assessed the efficiency of *Ddx3x* knockdown. Data are presented as means ± SEM. $^{***}p < 0.001$. (B) The protein level of DDX3X, Casp-3 and cleaved Casp-3 in H9c2 cells treated with Dox (2 μM) following *Ddx3x* siRNA transfection. Data are presented as means ± SEM. ns, $p \geq 0.05$ refers to not significant; $^{*}p < 0.05$; $^{**}p < 0.01$; $^{***}p < 0.001$. (C) Flow cytometric analysis detected the apoptosis ratio of H9c2 cardiomyocytes treated with Dox (2 μM) following *Ddx3x* siRNA transfection. The data are presented as means ± SEM. ns, $p \geq 0.05$ refers to not significant; $^{**}p < 0.01$. (D) Mito-Tracker Red CMXRos and Hoechst 33342 staining were detected respectively mitochondrial morphology and nuclear condensation of H9c2 cardiomyocytes treated with Dox (2 μM) following *Ddx3x* siRNA transfection. Scale bar = 50 μm. (E) The CCK-8 assay was used to detect cell viability of H9C2 cells treated with Dox (2 μM) following *Ddx3x* siRNA transfection. Data are presented as means ± SEM. ns, $p \geq 0.05$ refers to not significant; $^{*}p < 0.05$; $^{***}p < 0.001$. (F) The protein level of DDX3X, Casp-3 and cleaved Casp-3 in H9c2 cells treated with Dox (2 μM) following RK-33 pretreatment. Data are presented as means ± SEM. ns, $p \geq 0.05$ refers to not significant; $^{*}p < 0.05$; $^{**}p < 0.01$; $^{***}p < 0.001$. (G) Mito-Tracker Red CMXRos and Hoechst 33342 staining were detected respectively mitochondrial morphology and nuclear condensation of H9c2 cells treated with Dox (2 μM) following RK-33 pretreatment. Scale bar = 50 μm

determined using RT-qPCR. Compared with the negative control group, the mRNA expression level of DDX3X was increased in the *Ddx3x* plasmid transfection group (Figure 3A), indicating that DDX3X was successfully overexpressed in H9c2 cardiomyocytes. As shown in Figure 3B, *Ddx3x* overexpression remarkably reduced the activation level of Caspase-3 induced by Dox treatment in H9c2 cardiomyocytes. The results of flow cytometric analysis and Mito-Tracker Red CMXRos and Hoechst 33342 staining also suggested that *Ddx3x* overexpression largely reversed Dox-induced H9c2 cells apoptosis and mitochondrial damage (Figure 3C,D). No significant differences in the apoptosis ratio of H9c2 cells were observed between the *Ddx3x*-overexpressing and control groups without Dox treatment (Figure 3B–D). These results demonstrated that DDX3X upregulation notably attenuated H9c2 cardiomyocytes apoptosis induced by Dox treatment.

3.4 | DDX3X regulated DIC via the Wnt/β-catenin signaling pathway

It has been shown that DDX3X is a regulator of canonical Wnt/β-catenin signaling.[18] Western blot analysis was used to detect β-catenin protein levels in H9c2 cells after Dox treatment for the indicated time periods. We found that the protein level of β-catenin was decreased in H9c2 cells after exposure to Dox (Figure 4A), suggesting that the canonical Wnt/β-catenin signaling pathway was inhibited in DIC. In view of the Dox-induced downregulation of DDX3X, we speculated that DDX3X downregulation suppressed Wnt/β-catenin signaling in DIC. As expected, compared to the control group, *Ddx3x* knockdown exacerbated the decline in β-catenin protein levels in H9c2 cardiomyocytes treated with Dox (Figure 4B). In contrast, *Ddx3x* overexpression largely reversed the decrease in β-catenin levels triggered by Dox treatment (Figure 4C). Moreover, we aimed to determine whether DDX3X ATPase activity is involved in the regulation of Wnt signaling in DIC. As shown in Figure 4D, RK-33 pretreatment aggravated the reduction of β-catenin protein triggered by Dox treatment in H9c2 cardiomyocytes, indicating that the ATPase activity of DDX3X is implicated in regulating Wnt/β-catenin signaling. As shown in Figure 4E, LiCl pretreatment had no effect on DDX3X expression and largely reversed the decreased β-catenin protein level and increased Caspase-3 activation induced by Dox treatment and *Ddx3x* knockdown. The results of Mito-Tracker Red CMXRos and Hoechst 33342 staining also showed that LiCl pretreatment alleviated H9c2 cardiomyocyte apoptosis induced by Dox treatment (Figure 4F). These results indicate that the canonical Wnt/β-catenin signaling pathway plays a protective role in DIC and that DDX3X can regulate Wnt/β-catenin signaling to stabilize β-catenin protein levels and mitigate DIC.

4 | DISCUSSION

Dox exerts a broad spectrum of antitumor effects and is widely used as a first-line chemotherapy drug against various forms of cancers, but the cumulative dose-dependent cardiotoxic effect limits its clinical therapeutic utility.[20] To date, many studies have been conducted to decipher the underlying molecular mechanism by which Dox leads to myocardial injury, and a large number of mechanisms have been revealed, such as ROS generation, mitochondrial dysfunction, and apoptosis.[21] However, the precise biochemical mechanisms underlying Dox-induced cardiac dysfunction are still not fully elucidated but are very complicated and require further study.

DDX3X is an ATPase/RNA helicase of the DEAD-box family that participates in nearly all aspects of RNA metabolism.[22] In addition to regulating RNA metabolism, DDX3X plays roles in multiple biological processes, such as cortical development,[23] cell growth,[24] phase-separated organelle formation,[25] the NLRP3 inflammasome assembly,[26] viral replication,[27] innate immune response,[28] and apoptosis.[29] Dysfunction of DDX3X is associated with various diseases, such as neurodevelopmental disorders,[30] viral infection, cancer,[31–32] and inflammatory bowel disease.[33] In this study, we observed that DDX3X expression was reduced in H9c2 cardiomyocytes treated with Dox. Both *Ddx3x* knockdown and inhibition of DDX3X ATPase activity by RK-33 aggravated apoptosis and mitochondrial dysfunction in H9c2 cells treated with Dox. Conversely, *Ddx3x* overexpression mitigated DIC. These results suggest that DDX3X plays an important role in the pathological processes of Dox-induced cardiac dysfunction.

The Wnt/β-catenin signaling is one of the fundamental mechanisms regulating many biological developmental processes, including cell proliferation, differentiation, genetic stability, and cell fate specification during embryogenesis, organogenesis, and tissue homeostasis.[5–6] Multiple lines of evidence have implicated Wnt/β-catenin signaling in cardiovascular diseases, including myocardial infarction, cardiac hypertrophy, heart failure, and atherosclerosis.[34] The Wnt signaling is mostly silent under physiological conditions in the healthy adult heart but is generally reactivated under pathological conditions.[35] For instance, some components of the Wnt signaling pathway are upregulated following myocardial infarction, and the reactivation of Wnt/β-catenin signaling is conducive to myocardial infarct healing.[36–37] Moreover, it has been shown that the Wnt-GSK3-Akt-mTOR pathway participates in the regulation of cellular energy balance and metabolism and that the short-term and early activation of the Wnt-GSK3-mTOR axis could alleviate isoproterenol-induced cardiotoxicity in rodents.[38] Previous research has shown that secreted frizzled-related protein 1 (sFRP1) reduced infarct size and improved cardiac function by regulating Wnt/PCP-JNK signaling.[39] However, the role of Wnt/β-catenin signaling in DIC has not been well elucidated yet. In our study, we found that the protein level of β-catenin was remarkably decreased in H9c2 cells treated with Dox, suggesting that Wnt/β-catenin signaling was inhibited in DIC.

DDX3X is a positive regulator of the Wnt/β-catenin signaling pathway.[18] However, to date, the DDX3X-Wnt/β-catenin signaling axis has only been studied in oncological research.[40] In this study, we found that *Ddx3x* knockdown reduced β-catenin protein levels in H9c2 cells after Dox treatment and that *Ddx3x* overexpression partly reversed the decrease in β-catenin induced by Dox. Moreover,

LiCl pretreatment ameliorated mitochondrial injury in H9c2 cardiomyocytes and apoptosis induced by Dox treatment and *Ddx3x* knockdown, indicating that the activation of Wnt/β-catenin signaling plays a protective role in DIC. Therefore, we conclude that Dox-induced DDX3X downregulation contributes to the suppression of Wnt/β-catenin signaling, promoting mitochondrial injury and apoptosis of cardiomyocytes. Previous studies have demonstrated that DDX3X regulates Wnt signaling through an ATPase activity-independent mechanism.[18] However, in this study, RK-33, which inhibits the ATPase activity of DDX3X, exacerbated the decline in the

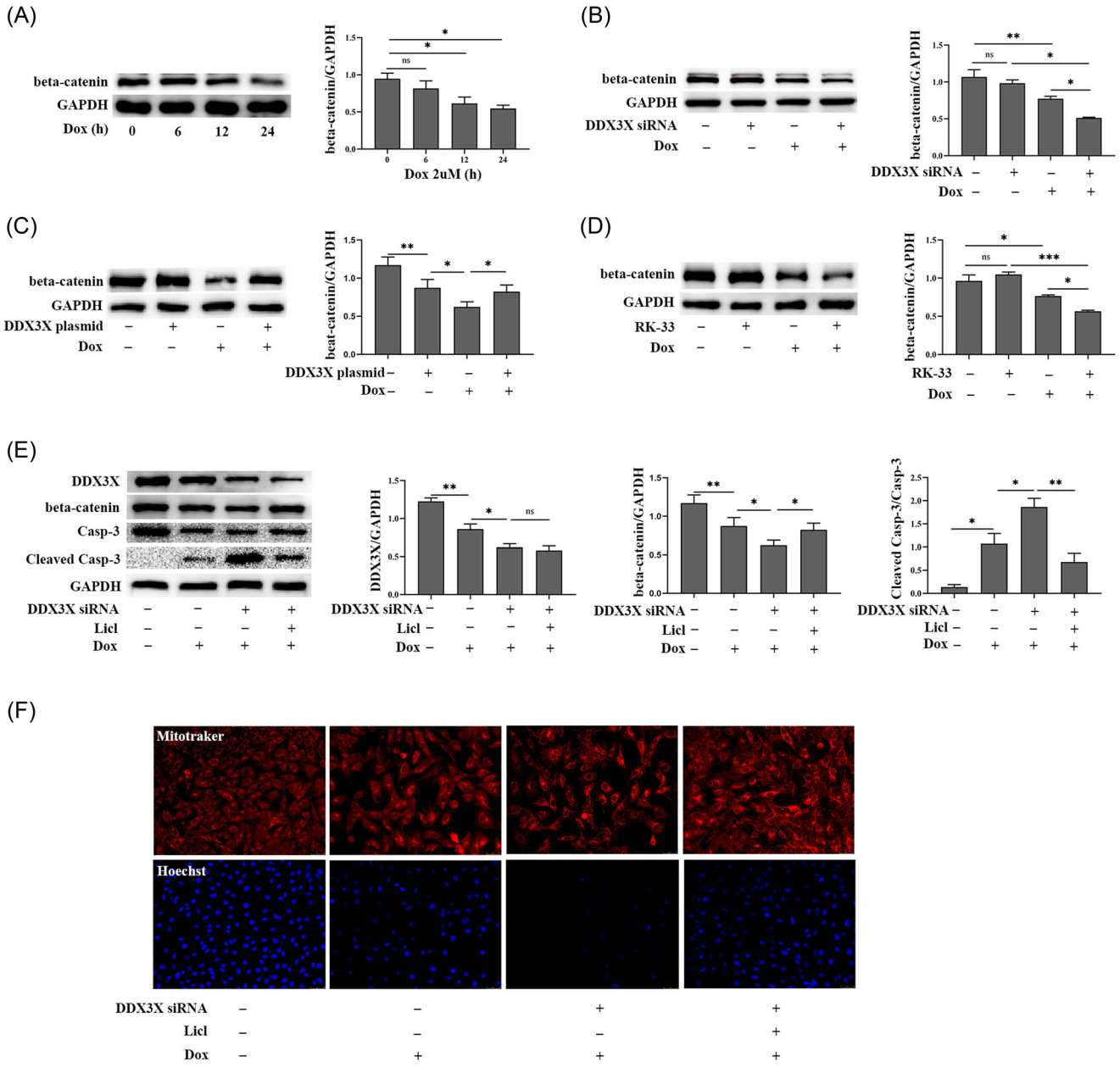

FIGURE 4 DDX3X regulated Dox-induced cardiotoxicity via canonical Wnt/β-catenin signaling pathway. "+" symbol denotes presence and "–" symbol denotes absence of the corresponding treatment condition. (A) The protein level of β-catenin in H9c2 cells treated with Dox (2 μM) for 0, 6, 12, and 24 h. Data are presented as means ± SEM. ns, $p \geq 0.05$ refers to not significant; $^{*}p < 0.05$. (B) The protein level of β-catenin in H9c2 cells treated with Dox (2 μM) following *Ddx3x* siRNA transfection. Data are presented as means ± SEM. ns, $p \geq 0.05$ refers to not significant; $^{*}p < 0.05$; $^{**}p < 0.01$. (C) The protein level of β-catenin in H9c2 cells treated with Dox (2 μM) following RK-33 pretreatment. Data are presented as means ± SEM. ns, $p \geq 0.05$ refers to not significant; $^{*}p < 0.05$; $^{***}p < 0.001$. (D) The protein level of β-catenin in H9c2 cells treated with Dox (2 μM) following *Ddx3x* plasmids transfection. Data are presented as means ± SEM. $^{*}p < 0.05$; $^{**}p < 0.01$. (E) The protein level of DDX3X, β-catenin, Casp-3, and cleaved Casp-3 in H9c2 cells treated with Dox (2 μM) following *Ddx3x* siRNA transfection and LiCl pretreatment. Data are presented as means ± SEM. ns, $p \geq 0.05$ refers to not significant; $^{*}p < 0.05$; $^{**}p < 0.01$. (F) Mito-Tracker Red CMXRos and Hoechst 33342 staining were detected respectively mitochondrial morphology and nuclear condensation of H9c2 cells treated with Dox (2 μM) following *Ddx3x* siRNA transfection and LiCl pretreatment. Scale bar = 0 μm

β-catenin protein levels in H9c2 cells treated with Dox, which suggests that DDX3X ATPase participates in the regulation of Wnt/β-catenin signaling in DIC.

In summary, this study is the first to show that DDX3X participates in DIC regulation. DDX3X upregulation attenuates DIC by activating Wnt/β-catenin signaling and promoting the stabilization and accumulation of cytosolic β-catenin in vitro. This finding helps us to identify a new perspective for understanding the mechanism of DIC. However, there were some limitations to our study because no in vivo data were provided. Further studies are necessary to confirm whether DDX3X is a potential therapeutic target for DIC.

AUTHOR CONTRIBUTIONS

Enkui Hao, Ju Liu, Jing Liu, and Dandan Feng conceived and supervised the study; Dandan Feng and Enkui Hao designed experiments; Dandan Feng, Jiang Li, Liang Guo, Xiuyuan Ma, Shaochen Wang, and Yunxuan Song performed experiments; Dandan Feng analyzed data; Dandan Feng wrote the manuscript; Enkui Hao, Ju Liu, Jing Liu, and Dandan Feng made manuscript revisions.

ACKNOWLEDGMENTS

This study was supported by the Science and Technology Project of Shandong Province (grant no. 11731303), the National Nature Science Foundation of China (grant no. 81873473), and the Academic Promotion Program of Shandong First Medical University (grant no. 2019QL014), Jinan City's Science and Technology Innovation Program of Clinical Medicine (grant no. 202019175).

CONFLICTS OF INTEREST

The authors declare no conflicts of interest.

DATA AVAILABILITY STATEMENT

The data that support the findings of this study are available from the corresponding author upon reasonable request.

ORCID

Enkui Hao http://orcid.org/0000-0001-8770-8076

REFERENCES

[1] C. A. Hudis, N. Schmitz, *Semin. Oncol.* **2004**, *31*(3), 19.
[2] C. F. Thorn, C. Oshiro, S. Marsh, T. Hernandez-Boussard, H. McLeod, T. E. Klein, R. B. Altman, *Pharmacogenet. Genom.* **2011**, *21*(7), 440.
[3] K. Chatterjee, J. Zhang, N. Honbo, J. S. Karliner, *Cardiology* **2010**, *115*(2), 155.
[4] Y. Octavia, C. G. Tocchetti, K. L. Gabrielson, S. Janssens, H. J. Crijns, A. L. Moens, *J. Mol. Cell. Cardiol.* **2012**, *52*(6), 1213.
[5] M. Kahn, *Nat. Rev. Drug Discovery* **2014**, *137*, 513.
[6] B. T. MacDonald, K. Tamai, X. He, *Dev. Cell* **2009**, *17*(1), 9.
[7] C. M. Warboys, N. Chen, Q. Zhang, Y. Shaifta, G. Vanderslott, G. Passacquale, Y. Hu, Q. Xu, J. P. T. Ward, A. Ferro, *Cardiovasc. Res.* **2014**, *104*(1), 116.
[8] S. Kaga, L. Zhan, E. Altaf, N. Maulik, *J. Mol. Cell. Cardiol.* **2006**, *40*(1), 138.
[9] G. Zu, J. Guo, N. Che, T. Zhou, X. Zhang, *Sci. Rep.* **2016**, *6*, 38480.
[10] V. Tajadura, M. H. Hansen, J. Smith, H. Charles, M. Rickman, K. Farrell-Dillon, V. Claro, C. Warboys, A, *Cell Death Dis.* **2020**, *11*(6), 493.
[11] M. W. Bergmann, C. Rechner, C. Freund, A. Baurand, A. El Jamali, R. Dietz, *J. Mol. Cell. Cardiol.* **2004**, *37*(3), 681.
[12] A. Jankowsky, U. P. Guenther, E. Jankowsky, *Nucleic Acids Res.* **2011**, *39*, D338.
[13] J. H. Park, Y. J. Jeong, K. K. Park, H. J. Cho, I. K. Chung, K. S. Min, M. Kim, K. G. Lee, J. H. Yeo, K. K. Park, Y. C. Chang, *Mol. Cells* **2001**, *12*(2), 209.
[14] W. J. Chen, W. T. Wang, T. Y. Tsai, H. K. Li, Y. H. W. Lee, *Sci. Rep.* **2017**, *7*(1), 9411.
[15] C. Foresta, *Hum. Mol. Genet.* **2000**, *9*(8), 1161.
[16] L. Snijders Blok, E. Madsen, J. Juusola, C. Gilissen, D. Baralle, M. R. Reijnders, H. Venselaar, C. Helsmoortel, M. T. Cho, A. Hoischen, L. E. Vissers, T. S. Koemans, W. Wissink-Lindhout, E. E. Eichler, C. Romano, H. Van Esch, C. Stumpel, M. Vreeburg, E. Smeets, K. Oberndorff, B. W. vanBon, M. Shaw, J. Gecz, E. Haan, M. Bienek, C. Jensen, B. L. Loeys, A. Van Dijck, A. M. Innes, H. Racher, S. Vermeer, N. Di Donato, A. Rump, K. Tatton-Brown, M. J. Parker, A. Henderson, S. A. Lynch, A. Fryer, A. Ross, P. Vasudevan, U. Kini, R. Newbury-Ecob, K. Chandler, A. Male, S. Dijkstra, J. Schieving, J. Giltay, K. L. vanGassen, J. Schuurs-Hoeijmakers, P. L. Tan, I. Pediaditakis, S. A. Haas, K. Retterer, P. Reed, K. G. Monaghan, E. Haverfield, M. Natowicz, A. Myers, M. C. Kruer, Q. Stein, K. A. Strauss, K. W. Brigatti, K. Keating, B. K. Burton, K. H. Kim, J. Charrow, J. Norman, A. Foster-Barber, A. D. Kline, A. Kimball, E. Zackai, M. Harr, J. Fox, J. McLaughlin, K. Lindstrom, K. M. Haude, K. van Roozendaal, H. Brunner, W. K. Chung, R. F. Kooy, R. Pfundt, V. Kalscheuer, S. G. Mehta, N. Katsanis, T. Kleefstra, *Am. J. Hum. Genet.* **2015**, *97*(2), 343.
[17] J. Mo, H. Liang, C. Su, P. Li, J. Chen, B. Zhang, *Mol. Cancer* **2021**, *20*(1), 38.
[18] C. M. Cruciat, C. Dolde, R. E. de Groot, B. Ohkawara, C. Reinhard, H. C. Korswagen, C. Niehrs, *Science (New York, N.Y.)* **2013**, *339*(6126), 1436.
[19] L. Meng, H. Lin, J. Zhang, N. Lin, Z. Sun, F. Gao, H. Luo, T. Ni, W. Luo, J. Chi, H. Guo, *J. Mol. Cell. Cardiol.* **2019**, *136*, 15.
[20] M. A. Fridrik, U. Jaeger, A. Petzer, W. Willenbacher, F. Keil, A. Lang, J. Andel, S. Burgstaller, O. Krieger, W. Oberaigner, K. Sihorsch, R. Greil, *Eur. J. Cancer (Oxford, England: 1990)* **2016**, *58*, 112.
[21] K. Renu, S. Arunachalam, *Eur. J. Pharmacol.* **2018**, *818*, 241.
[22] P. Linder, E. Jankowsky, *Nat. Rev. Mol. Cell Biol.* **2011**, *12*(8), 505.
[23] A. L. Lennox, M. L. Hoye, R. Jiang, B. L. Johnson-Kerner, L. A. Suit, S. Venkataramanan, C. J. Sheehan, F. C. Alsina, B. Fregeau, K. A. Aldinger, C. Moey, I. Lobach, A. Afenjar, D. Babovic-Vuksanovic, S. Bézieau, P. R. Blackburn, J. Bunt, L. Burglen, P. M. Campeau, P. Charles, B. H. Y. Chung, B. Cogné, C. Curry, M. D. D'Agostino, N. Di Donato, L. Faivre, D. Héron, A. M. Innes, B. Isidor, B. Keren, A. Kimball, E. W. Klee, P. Kuentz, S. Küry, D. Martin-Coignard, G. Mirzaa, C. Mignot, N. Miyake, N. Matsumoto, A. Fujita, C. Nava, M. Nizon, D. Rodriguez, L. S. Blok, C. Thauvin-Robinet, J. Thevenon, M. Vincent, A. Ziegler, W. Dobyns, L. J. Richards, A. J. Barkovich, S. N. Floor, D. L. Silver, E. H. Sherr, *Neuron* **2020**, *106*(3), 404.
[24] M. C. Lai, W. C. Chang, S. Y. Shieh, W. Y. Tarn, *Mol. Cell. Biol.* **2010**, *30*(22), 5444.
[25] M. Hondele, R. Sachdev, S. Heinrich, J. Wang, P. Vallotton, B. Fontoura, K. Weis, *Nature* **2019**, *573*(7772), 144.
[26] P. Samir, S. Kesavardhana, D. M. Patmore, S. Gingras, R. Malireddi, R. Karki, C. S. Guy, B. Briard, D. E. Place, A. Bhattacharya, B. R. Sharma, A. Nourse, S. V. King, A. Pitre, A. R. Burton, S. Pelletier, R. J. Gilbertson, T. D. Kanneganti, *Nature* **2019**, *573*(7775), 590.

[27] A. Brai, R. Fazi, C. Tintori, C. Zamperini, F. Bugli, M. Sanguinetti, E. Stigliano, J. Esté, R. Badia, S. Franco, M. A. Martinez, J. P. Martinez, A. Meyerhans, F. Saladini, M. Zazzi, A. Garbelli, G. Maga, M. Botta, *Proc. Natl. Acad. Sci. U.S.A.* **2016**, *113*(19), 5388.
[28] D. Soulat, T. Bürckstümmer, S. Westermayer, A. Goncalves, A. Bauch, A. Stefanovic, O. Hantschel, K. L. Bennett, T. Decker, G. Superti-Furga, *EMBO J.* **2008**, *27*(15), 2135.
[29] M. Sun, L. Song, Y. Li, T. Zhou, R. S. Jope, *Cell Death Differ.* **2008**, *15*(12), 1887.
[30] B. Johnson-Kerner, L. Snijders Blok, L. Suit, J. Thomas, T. Kleefstra, E. H. Sherr, *GeneReviews®*, University of Washington, Seattle, **2020**.
[31] Y. Ariumi, *Front. Genet.* **2014**, *5*(423), 1-10.
[32] L. Zhao, Y. Mao, J. Zhou, Y. Zhao, Y. Cao, X. Chen, *Am. J. Cancer Res.* **2016**, *6*(2), 387.
[33] S. Tantravedi, F. Vesuna, P. T. Winnard, M. Van Voss, P. J. Van Diest, V. Raman, *Oncotarget* **2017**, *8*(70), 115280.
[34] S. Foulquier, E. P. Daskalopoulos, G. Lluri, K. Hermans, A. Deb, W. M. Blankesteijn, *Pharmacol. Rev.* **2018**, *70*(1), 68.
[35] K. Kuwahara, K. A. Nakao, *J. Pharmacol. Sci.* **2011**, *116*(4), 337.
[36] S. Srivastava, N. Bagang, S. Yadav, S. Rajput, D. Sharma, A. Dahiya, L. Bhardwaj, K. Deshmukh, J. C. Joshi, G. Singh, *Inflamm Res.* **2021**, *70*(7), 743.
[37] Y. H. Hu, J. Liu, J. Lu, P. X. Wang, J. X. Chen, Y. Guo, F. H. Han, J. J. Wang, W. Li, P. Q. Liu, *Acta Pharmacol. Sin.* **2020**, *41*(9), 1150.
[38] L. Chen, Q. Wu, F. Guo, B. Xia, J. Zuo, *J. Cell. Mol. Med.* **2004**, *8*(2), 257.
[39] L. Barandon, T. Couffinhal, J. Ezan, P. Dufourcq, P. Costet, P. Alzieu, L. Leroux, C. Moreau, D. Dare, C. Duplàa, *Circulation* **2003**, *108*(18), 2282.
[40] F. Yang, E. Fang, H. Mei, Y. Chen, H. Li, D. Li, H. Song, J. Wang, M. Hong, W. Xiao, X. Wang, K. Huang, L. Zheng, Q. Tong, *Cancer Res.* **2019**, *79*(3), 557.

How to cite this article: D. Feng, J. Li, L. Guo, J. Liu, S. Wang, X. Ma, Y. Song, J. Liu, E. Hao, *J. Biochem. Mol. Toxicol.* **2022**;36:e23077. https://doi.org/10.1002/jbt.23077